Proc. SPIE **2869**, 1080-1083, 1997

Imaging White Light VISAR

David J. Erskine* and Neil C. Holmes
Lawrence Livermore Nat. Lab., Livermore CA 94550

An imaging white light velocimeter consisting of two image superimposing Michelson interferometers in series with the target interposed is demonstrated. Interferometrically measured 2-dimensional velocity maps can be made of moving surfaces using unlimited bandwidth incoherent and extended area sources. Short pulse and broadband chirped pulse lasers can be used to provide temporal resolution not possible with monochromatic illumination. A ∼20 m/s per fringe imaging velocimeter is demonstrated using an ordinary camera flash for illumination. Radial and transverse velocity components can be measured when the illuminating and viewing beams are non-parallel.
Keywords: velocity, interferometer, VISAR, white light, imaging, velocimetry

The interferometric measurement of velocities through the Doppler shift of reflected waves is an important and widespread diagnostic tool. In the shock physics community, this is done by Fabry-Perot or Michelson based velocimeters, the latter often called a VISAR. Until recently, velocimeters were restricted to the use of narrowband illumination. Gidon and Behar[1] introduced a double interferometer method that extended the practical bandwidth to several nanometers. Their technique however is limited by the angle dependence of the Fabry-Perot to pointlike light sources which can be collimated into parallel rays.

Recently, we presented[2] a method we call white light velocimetry that allows the use of an unlimited bandwidth source of extended area. The innovation is the use of what we call image superimposing interferometers, which imprint the same delay independent of ray angle, position and wavelength. With this technique any source can be used, including extended area incandescent lamps and multi-wavelength sets of lasers. Short pulse and chirped pulse lasers can be used for the first time to perform time-resolved velocity interferometry.

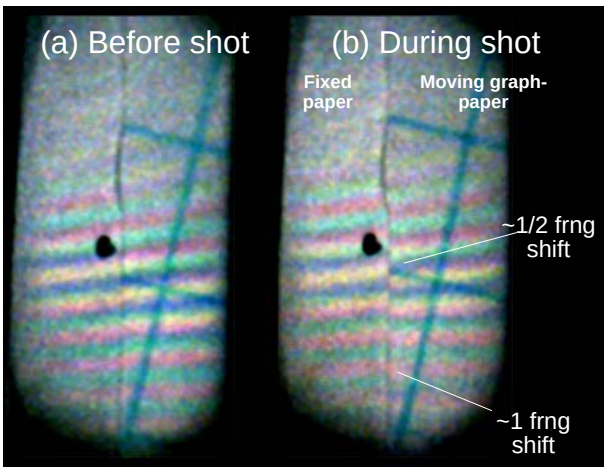

FIG. 1: Color photograph of multi-color fringes produced by the white light velocimeter prior (a) and during (b) a shot. The fringes were recorded on Kodak Royal 1000 color negative film. The illumination source was a small camera flash of 20 μs duration. The target was a stationary piece of white paper (left side with dot) overlapping non-uniformly moving graph paper behind it (right side with blue grid lines). The fringes on the graphpaper side have shifted vertically due to velocity. The shift varies with position (top to bottom) because of a velocity gradient. The measured velocity map is shown in Fig. 4.

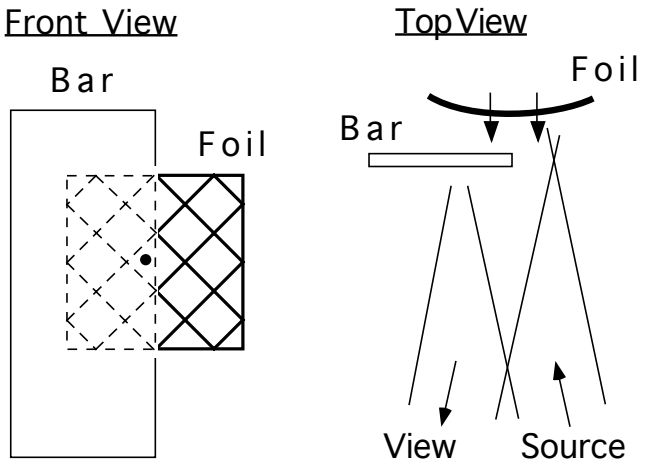

FIG. 2: Target configuration. Target was a ∼25 mm square aluminum foil propelled by a spark behind its center toward a stationary bar. A white piece of graph paper with 1/4 inch (6.4 mm) blue grid was glued to foil front. The foil was clamped more strongly at the top edge, resulting in a velocity which varies across the surface. A bar with white paper overlaps the foil and provides a stationary surface for reference. A small dot indicated the approximate axis of spark.

When the illuminating and viewing beams are collinear the velocity measured is a radial velocity. A transverse component can be measured by non-parallel viewing and illuminating beams. The 3-dimensional velocity vector can be reconstructed by the use of several viewing beams.

Broadband illumination allows unambiguous determination of the zeroth fringe, so that the fringe phase can be tracked through discontinuous velocity histories, such

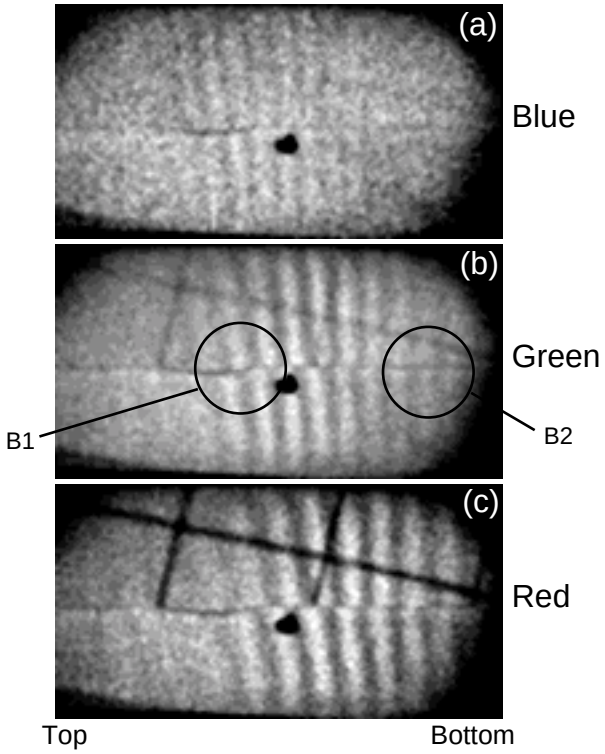

FIG. 3: The red, green and blue emulsion components of Fig. 1, for the shot. The fringe comb spacing is proportional to average wavelength of sensitivity for the given film emulsion component. The fringe shift at position B1 is approximately 0.5 and at position B2 approximately unity. Analysis shows the velocity increasing from 3 m/s to 20 m/s from left to right side of the image. Uncompensated interferometer dispersion causes the center of the fringe pattern to differ for different colors. The fringe contrast is poorer for blue because the spherical mirror coating is not ideally reflective, causing the interferometer arms to have unequal intensities for blue.

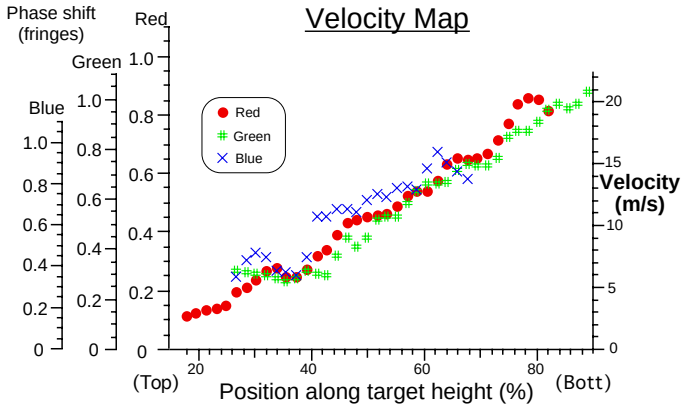

FIG. 4: Phase shift and corresponding deduced velocity along the height of the target at the edge between graph-paper and plane-paper sides. Information from the red, green and blue (RGB) emulsions is redundant in the details of the phase, but unique in determining the integer order. The change in fringe position on the graphpaper side of target before and after the shot was measured. Slight change on stationary side (due to table vibration) was accounted for. Factory derived values for the average wavelengths of the RGB emulsions were used, 633, 540, and 446 nm respectively. A better agreement for blue could have been obtained if this was an adjustable parameter. The velocity is obtained from each fringe shift using Eq. 1 and τ=13.33 ns.

as found in the measurement of shock waves. It produces optimal resolution of debris having different velocities but overlapped in view of the detector, such as debris from a disintegrating target. For targets which can have an unanticipated or evolving albedo spectrum, broadband illumination increases the likelihood of a reflected signal of significant intensity. The use of chirped illumination with a diffraction grating on output creates an all-optical streak camera capable of measuring motion over a line image with picosecond resolution[3]. Finally, the white light velocimeter allows the use of extended incoherent sources which are attractive for their convenience, compactness, cost or large total energy for illuminating a wide area.

Figure 1 is a color photograph of the multicolor fringes produced by the white light velocimeter prior to and during a shot. Figure 3 shows the red, green and blue (RGB) components of Fig. 1 for the shot. Figure 2 shows that the target consists of stationary and moving sheets of white paper in the same field of view. Thus, this constitutes a discontinuous non-uniformly moving target. In addition, the graphpaper side of the target is moving non-uniformly in a continuous manner, because one edge of the surface was more strongly clamped than the opposite edge. A plot of red, green, and blue fringe shifts (Fig. 4) indicates the velocity grows from 3 m/s to 20 m/s from the left to right of Fig. 3.

The illumination source was a small camera flash. This contrasts with conventional velocimetry where monochromatic and pointlike (laser) illumination is used. Secondly, conventional VISAR velocimetry is usually non-imaging, measuring velocity at a single or several points, or at most along a line. (Imaging Fabry-Perot velocimetry has been accomplished[4].) This experiment is therefore notable because it demonstrates an imaging capability, the use of wideband incoherent and extended source of light, and the recording of a target having a velocity gradient across its surface.

Figure 5 is a line diagram depicting the white light velocimeter (WLV) method. Two image superimposing interferometers are used in series with the target interposed. The interferometers are labeled "source" and "viewing", and have delays τ_1 and τ_2, respectively, which must nearly match. The superimposing condition requires that for a given interferometer, all images created by the interferometer superimpose longitudinally, transversely and in magnification, even though there is a temporal delay between the rays. This produces an interferometer delay which is independent of ray angle, for each

image pixel.

The two interferometers can either be physically distinct, as in this demonstration, or can be realized by the same optics if the illumination retro-reflects from the target, as demonstrated in Ref. 2. The latter configuration is the simplest because the delays τ_1 and τ_1 are automatically matched. However, separate interferometers may be desired to eliminate glare from shared optics so that weak reflectors can be observed, and so that one interferometer can be aligned differently than the other to form a fine fringe comb across the target image. Separate interferometers also allow a large field of view useful for imaging velocimetry, which is the interest here.

If the delays τ_1 and τ_2 match within the coherence length of the source, then partial fringes are formed whose phase depends on $(\tau_1 - \tau_2)$. Let $\tau = \tau_1 \approx \tau_2$ be the gross delay value. The velocity per fringe sensitivity η is given approximately by

$$\eta = \langle\lambda\rangle/2\tau \tag{1}$$

where $\langle\lambda\rangle$ is the average wavelength of the light being detected. Equation 1 is used to choose the general size for τ, which can range from $c\tau = 1$ mm to 10 meters for applications ranging from plasma physics to windtunnel diagnostics, where c is the speed of light.

The production of fringes can be explained either in the time domain, as in Ref. 2, or in the frequency domain, as is done here. Consider each interferometer to be a comb filter with sinusoidal pass bands periodically spaced $1/\tau$ apart, in frequency space. The target velocity through the Doppler effect causes the source interferometer comb spectrum to scale by a factor $(1 + 2v/c)$, where v is the target velocity for normal incidence and c is the speed of light. As the velocity changes, the overlap between the two slightly different comb filters produces fluctuations in the intensity passing through both interferometers, integrated over the range of wavelengths detected. This is analogous to Moiré fringes from two overlaid meshes having slightly different pitches.

For Michelson superimposing interferometers, the time averaged output intensity I from the viewing interferometer in the region of fringes varies approximately sinusoidally above a constant background as

$$\Delta I = \cos[\frac{2\pi}{\lambda}c(\tau_1 - \tau_2) - \frac{2\pi}{\lambda}(c\tau_1)\frac{2v}{c} + \phi_0] \tag{2}$$

where ΔI is the fluctuating part of the time averaged intensity, and ϕ_0 is some phase constant. The average wavelength is often determined by the detector. For example, in our case by the sensitivity spectra of the red-, green- or blue- emulsions in color film.

A single channel wideband detector could be used to record intensity. However, it is preferable to use a multichannel detecting system where channels are organized either by wavelength or delay difference $(\tau_1 - \tau_2)$. Both methods are used in this demonstration. By slightly misaligning a viewing interferometer mirror, the delay difference is made to vary across the image. Then target velocity causes the fringe comb to displace transversely across the image. In addition to this, the use of color film creates a 3-channel recording organized by wavelength.

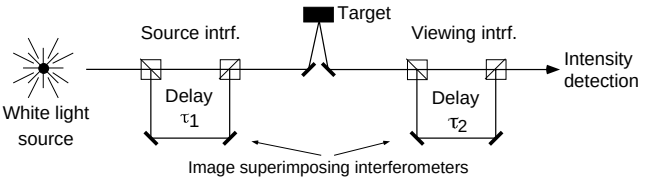

FIG. 5: Line diagram of a white light velocimeter. The parallelograms represent generic image superimposing interferometers. If interferometer delays τ_1 and τ_2 match within a coherence time of the source, partial fringes are produced at the output which vary with $(\tau_1 - \tau_2)$. Target velocity scales the apparent value of τ_1 due to the Doppler effect, changing the fringe phase.

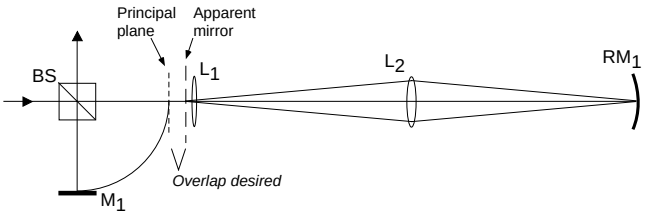

FIG. 6: A Michelson superimposing interferometer. In actuality, an equivalent spherical reflector is substituted for L_2. The principal plane is the reflection of M_1 seen in the beamsplitter BS. The apparent mirror surface is the surface of spherical reflector RM_1 imaged by L_2 and L_1. To achieve full WLV capabilities, the apparent surface should overlap the principal plane for as many input ray angles, positions and wavelengths as possible.

Alternatively, a grating could be used to diffract a line or point image into a spectrum. Equation 2 indicates that fringes will be observed which are sinusoidal versus $1/\lambda$. When this configuration is used with a chirped pulse, a correspondence is made between wavelength and time at the target. This forms an optical streak camera[3] which measures velocity history along a line across the target.

The interferometers can be of a Michelson class (generating two images) or Fabry-Perot class (infinite series of images of decreasing intensity). Single monochromatic superimposing Michelson interferometers realized by an etalon in one arm have been used in VISAR velocity interferometers for many years[5,6]. These satisfy the superimposing condition only for one wavelength due to dispersion in the etalon, and thus are unsuitable for white light usage for long delays. The spherical aberration produced by the etalon can also be a concern if high numerical aperture imaging is desired. An example of a non-superimposing interferometer is the conventional Fabry-Perot, which longitudinally displaces the successive output rays for a given input ray. A Fabry-Perot can be

made superimposing by adding a positive lens internal to the cavity so that there is exactly +1 magnification per round trip.

The achromatic superimposing Michelson interferometer used in this demonstration uses a relay lens system in one arm. This is shown in Fig. 6, except that a transmissive lens L_2 represents the spherical mirror actually used. The interferometer delay is given by the path length difference between the two arms. Lenses L_2 and L_1 image the surface of a spherical reflector RM_1 to a so-called apparent mirror surface. This must superimpose with the image of M_1 seen in the beamsplitter BS, and which is called the principal plane. The goal of the interferometer is to superimpose the apparent mirror and principal plane surfaces for a wide range of incident ray angles, positions and wavelengths. Other lenses, not shown, relay the principal plane to the target.

The interferometers of our apparatus have 4 meter delays so that the velocity per fringe proportionality for white light is about 20 m/s. This allows the use of low velocity targets safe for tabletop demonstrations.

Post-publication notes: Relevant patents include Refs. 7–11. A method of measuring position and velocity simultaneously with broadband illumination is discussed in Ref. 9, and a method of creating broadband coherent delays of long duration for microwave signals is discussed in Ref. 10. Optical interferometers having long delays useful for white light imaging velocimetry are described in Ref. 11.

Acknowledgments

This work was performed under the auspices of the U.S. Department of Energy by the University of California, Lawrence Livermore National Laboratory under contract No. W-7405-Eng-48.

---

* erskine1@llnl.gov

[1] S. Gidon and G. Behar, "Multiple-line laser doppler velocimetry," *Appl. Opt.* **27**, pp. 2315–2319, 1988.

[2] D. Erskine and N. Holmes, "White light velocimetry," *Nature* **377**, pp. 317–320, 1995.

[3] A simple argument estimates the time resolution of a chirp illuminated streak system to be $\Delta t = \sqrt{T_p/(f_2 - f_1)}$, where T_p is the pulse duration having a range of frequencies f_1 to f_2.

[4] S. Gidon and G. Behar, "Instantaneous velocity field measurements: application to shock wave studies," *Appl. Opt.* **25**, pp. 1429–1433, 1986.

[5] W. Hemsing, "Velocity sensing interferometer (visar) modification," *Rev. Sci. Instr.* **50**, pp. 73–78, 1979.

[6] L. Barker and K. Schuler, "Correction to the veocity-per-fringe relationship for the visar interferometer," *J. Appl. Phys.* **45**, pp. 3692–3696, 1974.

[7] D. Erskine, "White light velocity interferometer," *US Patent* **5,642,194**, 1997.

[8] D. Erskine, "White light velocity interferometer," *US Patent* **5,910,839**, 1999.

[9] D. Erskine, "Noise pair velocity and range echo location system," *US Patent* **5,872,628**, 1999.

[10] D. Erskine, "Multichannel heterodyning for wideband interferometry, correlation and signal processing," *US Patent* **5,943,132**, 1999.

[11] D. Erskine, "Single and double superimposing interferometer systems," *US Patent* **6,115,121**, 2000.